ACS OMEGA

Article

Cite This: ACS Omega 2018, 3, 10999−11008

http://pubs.acs.org/journal/acsodf

Low-Energy Encapsulation of α-Tocopherol Using Fully Food Grade Oil-in-Water Microemulsions

M. Ali Aboudzadeh,[†] Ehsan Mehravar,[†] Mercedes Fernandez,[†] Luis Lezama,[‡,§] and Radmila Tomovska*[,†,∥]

[†]POLYMAT, University of the Basque Country, UPV/EHU, Joxe Mari Korta Center, Avda. Tolosa 72, 20018 Donostia-San Sebastián, Spain

[‡]Departamento de Química Inorgánica, Universidad del País Vasco UPV/EHU, B° Sarriena, 48970 Leioa, Spain

[§]BC Materials, Basque Center for Materials, Applications & Nanostructures, UPV/EHU Science Park, B° Sarriena, 48970 Leioa, Spain

[∥]Ikerbasque, Basque Foundation for Science, 48013 Bilbao, Spain

Supporting Information

ABSTRACT: Encapsulation of active agents, such as vitamins and antioxidants, is one of the possibilities that allow their incorporation in beverages, food, or in pharmaceutical products. Simultaneously, encapsulation protects these active agents from oxidation, producing more stable active compounds. Formation of nanodroplets by spontaneously formed microemulsion (ME) offers, on one hand, a low-energy technology of encapsulation and, on the other hand, because of a small size of the droplets, it assures long-term stability even in harsher environments. In this study, oil-in-water MEs allowed the low-energy encapsulation of α-tocopherol (αToc) into an aqueous medium with the aid of fully food-grade ingredients, using isoamyl acetate as the dispersed oil phase, which was selected between three different types of oils. Both cosurfactant-free and cosurfactant-holder ME systems were formulated, in which Tween 20 and glycerol were employed as the surfactant and the cosurfactant, respectively. The ME monophasic area was determined through the construction of pseudoternary phase diagrams. The encapsulated αToc within 10−20 nm nanocapsules showed radical scavenging activity dependent on the encapsulated amount of αToc, as it was demonstrated by electron paramagnetic resonance spectroscopy. The radical scavenging activity slightly increased within the time investigated, indicating a slow release of the active compound from the nanodroplets, which is a promising result for their application, especially in pharmaceuticals.

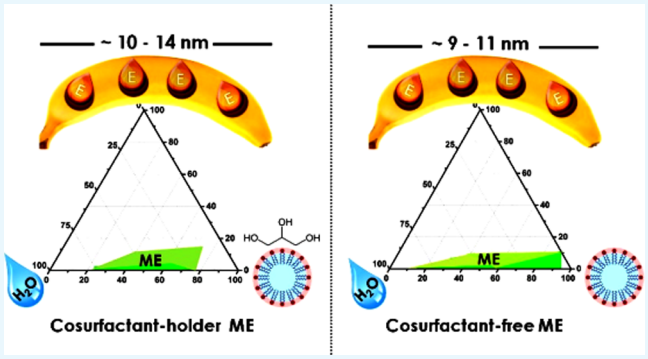

1. INTRODUCTION

There is a growing interest within the pharmaceutical and food industries to protect sensitive oil-soluble bioactive compounds such as vitamins in order to increase the public sanitation grades.[1−6] Encapsulation processes of the bioactive compounds allow their protection and delivery in a controlled manner and within a controlled environment.

Microemulsions (MEs), being the most dispersed of all, are particularly interesting as colloidal delivery systems because they can easily be created from food-grade ingredients using relatively simple processing protocols. ME is a single optically isotropic and thermodynamically stable liquid solution made of oil, water, surfactant, and mostly cosurfactant. It is one of the favorable delivery systems applied to increase the solubility of phytochemicals, nutraceuticals, and food additives.[7−11] MEs are normally easy to prepare without addition of high energy, providing them an excellent prospective of scaling-up and a financial advantage for industrial applications.[12] Additionally, ME offers encapsulation of the active agents within nanosized (<100 nm) capsules, which has been reported to favor the stability, duration, and interactions with different matrixes, facilitating controlled release and protecting the bioactive components.[13]

It has been widely reported that no single strategy of encapsulation is suitable for each kind of lipophilic component, and each colloidal system must be designed individually.[14] Therefore, the main aim of this work is to develop a ME system for encapsulation of relatively hydrophobic antioxidant compounds using completely food-grade ingredients. Different types of biobased oils as the solvent for bioactive compounds were studied in combination with a food-grade surfactant such as Tween 20 and vegetal glycerol as a cosurfactant. α-

Received: June 7, 2018
Accepted: August 7, 2018
Published: September 11, 2018

DOI: 10.1021/acsomega.8b01272
ACS Omega 2018, 3, 10999−11008

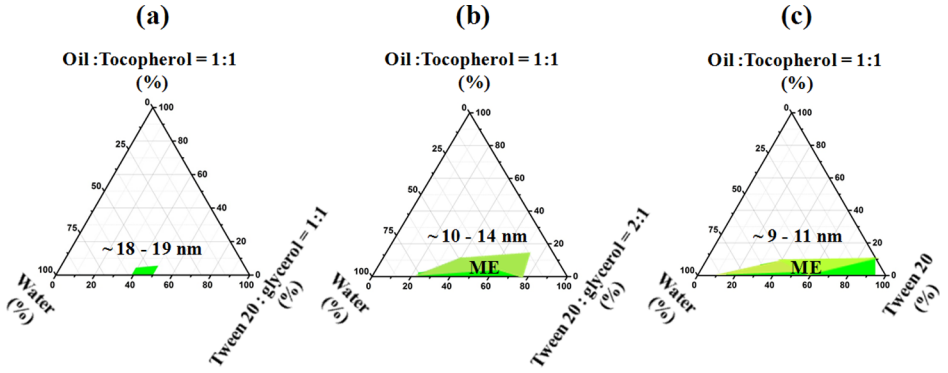

Figure 1. Pseudoternary phase behaviors of the system (IAAc + αToc)/(Tween 20, glycerol)/water at 25 °C. The weight ratio of Tween 20 to glycerol is 1:1 (a), 2:1 (b), and 1:0 (c). The oil to surfactant ratios were set at 1:9 and 2:9 levels. The ME regions are labeled in green, and the approximate droplet size obtained by DLS measurements are written above these regions.

Tocopherol (αToc) was selected as the model compound because it is one of the most studied antioxidants from the group of oil-soluble vitamin tocopherols, known by the common name of vitamin E.[15] It has superior bioavailability and the human body absorbs and metabolizes this form of vitamin E better than the others.[16,17] αToc, as the most important oil-soluble antioxidant, protects membranes from oxidation by reacting with lipid radicals produced in the lipid peroxidation chain reaction.[18−20] This removes the free radical intermediates and stops the propagation reactions, yielding oxidized α-tocopheroxyl radicals that may be further activated via reduction by other antioxidants, such as ascorbate, retinol, or ubiquinol.[21,22]

However, αToc as a functional ingredient is highly susceptible to oxidizing agents, turning dark and losing out the activity when exposed to air, heat, and light.[23−27] Moreover, because of its oily structure, it is water-insoluble; thus, it is essential to protect it against degradation and to convert it into easier-to-use forms. αToc has been widely encapsulated and prepared in different forms, such as nanoemulsions,[28−32] liposomes,[33,34] and nanoparticles.[25,35,36] Encapsulation of vitamin E has been reported to improve its physicochemical stability during storage time, in addition to its biological activity after consumption.[31,37] Use of ME to encapsulate vitamin E has an additional advantage because of the presence of a high amount of surface active compounds that enhance transdermal drug permeability and transmembrane passage across the alimentary tract; consequently, the bioavailability of vitamin E in oil-in-water (O/W) ME systems has been reported to be enhanced.[38−41]

The ME approach has widely been used in nanoencapsulation of bioactive compounds in general[42,43] and for nanoencapsulation of αToc in particular.[38,44−47] However, completely edible systems were reported only in two of them, up to the authors' best knowledge.[38,44] In order to complement these few pioneering studies in which the main focus was on the relationship between the structural design of the ME and the properties of the colloidal dispersions, herein we presented a simplified approach to encapsulate αToc in ME systems. In this approach, in addition to using a cosurfactant in the formulation of our αToc-loaded MEs, cosurfactant-free ME systems were developed, too. The elimination of one component from already complex ME formulations may be an onward step toward commercial application. Nanodroplet size was obtained in both cases (10−20 nm), which indeed provides an excellent long-term stability of the colloidal dispersions and protects the encapsulated αToc against degradation. Moreover, the radical scavenging capacity of the encapsulated αToc was demonstrated by electron paramagnetic resonance (EPR) spectroscopy,[48−50] indicating a slow release of the encapsulated αToc. This investigation is one step forward toward the development of enriching αToc water-soluble products for application in food, beverage, and especially pharmaceutical industries.

2. RESULTS AND DISCUSSION

2.1. Pseudoternary Phase Diagrams. As the main aim of the ME formulation for encapsulation of αToc is its application in food, beverage, and pharmaceutical industries, the choices of surfactant and cosurfactant have to meet the constraints issued from the current regulations for food formulations as well as the economic viability for the food industry. In the present work, the nonionic surfactant Tween 20 was selected as an ingredient for food-grade ME processing. Low toxicity potential, lack of irritation, and its ability to form stable emulsions are the main advantages of using this surfactant.[14,51,52] Nevertheless, MEs were stabilized by an interfacial film of surfactant molecules, mostly together with a cosurfactant in order to decrease the interfacial tension substantially. Considering the potential cosurfactants, neutral vegetable glycerol has been selected, as it had been used in the past instead of water for further improvement of the bioactive molecule protection and solubility.[53,54] To select an oil with the best performance for the creation of stable O/W MEs, three different oils were studied: lemon oil, ispropyl myristate (IPM), and isoamyl acetate (IAAc).

To understand the phase behavior and the transition boundaries of the present multicomponent ME system, the pseudoternary phase diagrams were created. Figure S1 shows the pseudoternary phase diagrams of the blank MEs for all the tested oils in the absence of the active agent (αToc). Each row of this figure belongs to an identical oil, whereas each column represents a different ratio between Tween 20 and glycerol, including 1:1; 2:1; and 1:0.

Almost in all the cases, relatively small areas of stable MEs were obtained. It is widely regarded that the weight ratio of the surfactant to the cosurfactant is one of the key elements that affects the area of the ME region.[55,56] For all the studied oils, the ME area increased slightly by decreasing the cosurfactant amount and reached the maximum in the case of the cosurfactant-free system (the last column of Figure S1). This behavior, although it was unexpected, can be explained by the

DOI: 10.1021/acsomega.8b01272
ACS Omega 2018, 3, 10999−11008

reported strong repulsive interactions between Tween 20 and glycerol, which causes the low coverage of the oil−water interface at the junction of the surface domains of both active compounds.[57] Thus, eliminating the cosurfactant in the present system resulted in higher coverage of the oil−water interface area, more effective emulsification, and growth of the ME area as shown in Figure S1.

Figure S1 also shows that the type of oil influences significantly the phase behavior in the presented systems. The molar volume of the oil phase, determined by its molecular weight and density, seems to have an important influence on the phase behavior of the system, as it determines the extent of the penetration of the oil within the surfactant hydrophobic tails. Therefore, the oil with long molecular chains and extended chemical structures will penetrate less within the surfactant.[58] Among the investigated oils, IAAc formed the greatest ME area (Figure S1c). Lower molecular weight (130.18 g mol^{-1}) and higher density (876 kg m^{-3}) of IAAc in comparison to the other two oils obviously allowed it to interact better with the surfactant. IAAc has been used as a food flavor for a long time because of its banana aroma. Therefore, it is considered to be a kind of "safe oil" and was selected as the oil phase in further experiments of the present work for encapsulation of αToc.

The effect of addition of αToc dissolved in IAAc (50 wt %) within the ME formulation on the phase behavior of the systems was further examined in the case of IAAc as the oil phase for each previously studied Tween 20/glycerol ratio. The corresponding pseudoternary phase diagrams are presented in Figure 1. The presence of αToc decreased the areas of stable MEs in comparison to αToc-free systems (Figure S1c), which likely happened because of the increased interface tension between the phases and as a result of replacing 50 wt % of the oil with a more hydrophobic component (αToc) within the ME formulations. Nevertheless, the effect of the Tween 20/glycerol ratio was not changed by the presence of αToc, and a decreasing glycerol concentration resulted in systems that are more colloidally stable.

The formulations of the stable mixtures containing αToc are presented in Table S1, whereas in Figure S2 the photos of all mixtures are shown, presenting the appearance of all samples after overnight mixing under ambient conditions. It can be observed that mostly viscous mixtures were formed for the water content within the range of 8.5−33 wt %. For water contents higher than 33 wt %, the mixtures were clear because of the effect of the added water that swelled within hydrophilic Tween 20 heads and increased the distance between the polyoxyethylene groups of Tween 20.[59]

Figure 1a depicts the phase diagram in which the Tween 20/glycerol ratio is 1:1. Out of the 16 samples prepared at this ratio, only two samples as presented in Table S1 were found to form a stable O/W ME containing 4.3−5.5 wt % of the oily phase, 44.5−56.5 wt % of the aqueous phase, and 39−50 wt % of a mixture of Tween 20 and glycerol. The other samples prepared presented phase separation or a gel structure (Figure S2) or they even formed a clear and stable liquid, but their droplet size [measured by dynamic light scattering (DLS)] was >100 nm.

When the Tween 20/glycerol ratio was set at 2:1 (Figure 1b), a larger ME domain was obtained. In this case, the corresponding weight concentration ranges of the components were: oil phase 3.45−11.15 wt %, aqueous phase 16.26−65.65 wt %, and surfactant 30.9−75 wt % (Table S1). To load a higher amount of αToc, the oil content in the ME must be as high as possible, but the increase in the oil concentration may cause instability and requires more surfactants, increasing the total cost as well as the oral insecurity.[60] In this work, the maximum oil amount of 11.15 wt % was emulsified in a stable O/W ME by employing 31 wt % of Tween 20 and 15.5 wt % of glycerol. On the basis of previous reports for minimizing the effect of the surfactant,[61] this amount of Tween 20 was considered safe and the respective ME composition was selected for further study.

For the glycerol-free system (Figure 1c), the results clearly showed that this system had the largest ME region as already explained. Among the 16 samples formulated in this category, six samples showed a phase separation or formed a gel (Figure S2), and the rest of them were obtained as clear and stable liquids, presenting a droplet size < 100 nm. Table S1 shows that for this system, the amount of aqueous phase required to form a stable ME varied from 19.5 to 83.3 wt % and that the maximum amount of oil emulsified was 8.35 wt %. Further increase of the oil content up to 10 wt % was possible only for an elevated amount of surfactant, as the water content in this formulation was only 9 wt %.

2.2. Physicochemical Properties of the Prepared αToc-MEs. To study the effect of MEs' composition on their structural characteristics, the droplet size was monitored by DLS for both blank and αToc-loaded MEs, and the results are shown in Table S1. The average droplet size of a ME may fall in the range of 5−100 nm.[62] DLS measurements revealed that the mean droplet sizes of an αToc-free (blank) ME were in the range of 7.53−10.17 nm and the droplet size distribution was monomodal [the polydispersity index (PDI) values were very low as shown in Table S1]. The transmission electron microscopy (TEM) images in Figure 2 present a more

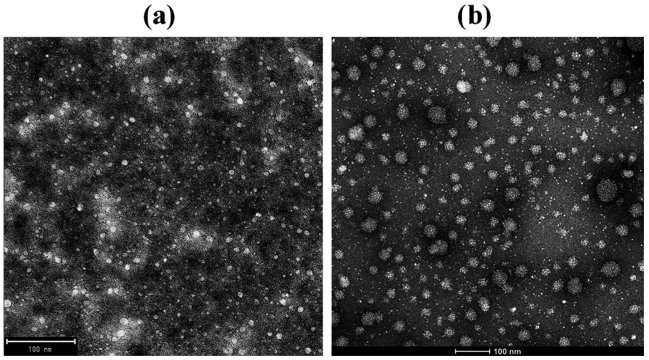

Figure 2. TEM images of sample 6 in αToc-free (a) and αToc-holder (b) MEs.

significant droplet size increase after αToc addition (up to 50 nm) than that obtained by DLS measurements (Table S1). However, by more careful observation, it is obvious that the larger droplets consist of a few smaller droplets' coalescent, which likely occurred because of the sample preparation for TEM measurements (droplet cast method). Therefore, it was considered that TEM images confirmed the findings observed from DLS.

Figure 2 shows TEM images of a representative αToc-free ME (sample 6, Table S1) and the corresponding αToc-holder ME. In both MEs, the oil droplets appeared well-dispersed without any aggregation or clusters and in a nanosize scale with a relatively narrow distribution. The αToc-free system (Figure

DOI: 10.1021/acsomega.8b01272
ACS Omega 2018, 3, 10999−11008

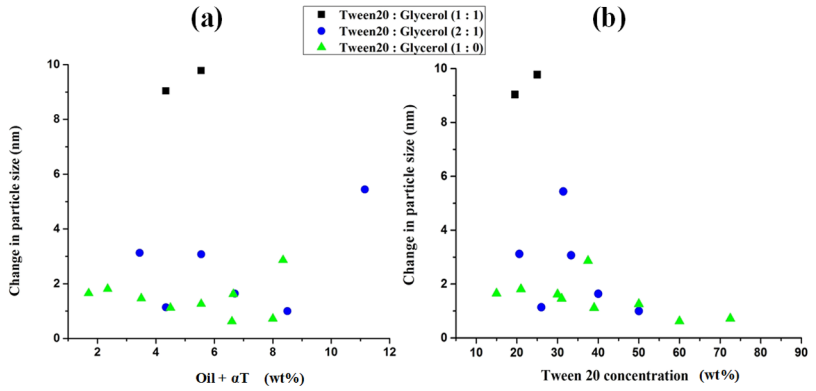

Figure 3. Effect of the oil phase (a) and surfactant (b) concentration on the droplet size increment after addition of αToc to ME at 25 °C. See Table S1 for the formulation details.

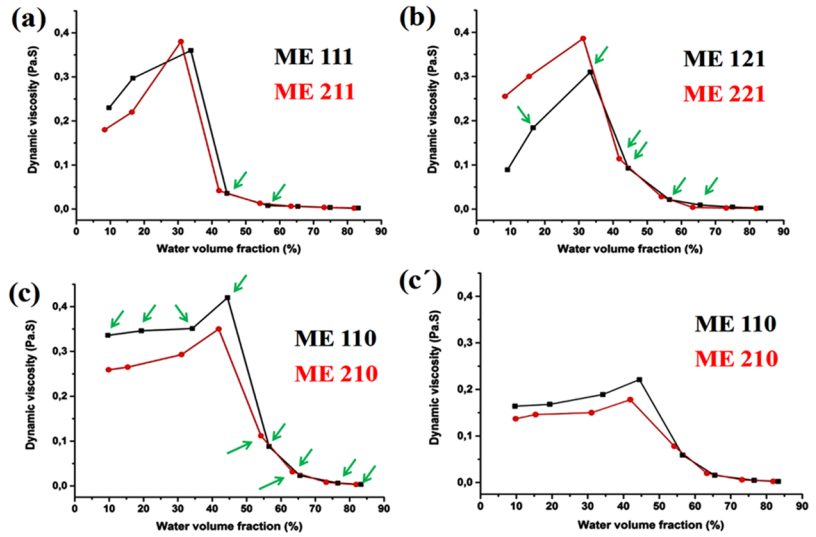

Figure 4. Dynamic viscosity as a function of the water volume fraction. Oil to surfactant phase ratio 1:9 (black curve) and 2:9 (red curve). (a) Tween 20/glycerol = 1:1 at 25 °C, (b) Tween 20/glycerol = 2:1 at 25 °C, (c) glycerol-free system at 25 °C and (c′) glycerol-free system at 37 °C. Green arrows depict stable MEs.

2a) contains a double amount of oil (4.35 wt %), and thus presented a higher number of droplets than the αToc-loaded system with an oil content of 2.18 wt % (Figure 2b). Incorporation of αToc into MEs affected the droplet size. Specifically, the droplet size of an αToc-loaded ME was considerably larger than that of an αToc-free ME, which was consistent with the data shown in Table S1. In Figure 3a,b, the increase in average droplet size after addition of αToc to blank ME as a function of oil and surfactant concentration is shown. The hydrophobic nature of αToc molecule caused augmentation of the interface tension of the system, which consequently resulted in average droplet size increment. The observed effect is the lowest (<2 nm) for the glycerol-free system and increased with glycerol addition and by rising its content; thus, the highest droplet size increment of almost 10 nm was obtained at a Tween 20/glycerol ratio of 1:1.

These results are in accordance with the largest ME areas obtained for the glycerol-free systems in phase diagrams (Figures 1 and S1) and confirmed the selection of the surfactant with an appropriate hydrophilic-lipophilic balance (HLB) for the system. Increase of the oil phase content in the ME formulation resulted in a higher increment of droplet size as the content of the Tween 20 decreased simultaneously (Figure 3a), an effect that has already been reported in literature.[63] The augmentation of surfactant content (Figure 3b) first resulted in a high increment of the droplet size because of a simultaneous increase of the dispersed phase and the decrease of water content. However, the droplet size slowly dropped for higher loads of the surfactant, and in the region of high surfactant loads (and very low water content), preferably water became the dispersed phase and this caused the droplet size to decrease.

These results demonstrate that in the developed ME formulation, the size of the nanodroplets could be varied rather in a narrow range by variation of the loads of individual components. These effects are minimized in glycerol-free systems.

The dependence of dynamic viscosity on the water volume fraction (W_0) may indicate the structural transitions in dispersed systems.[54,64] Figure 4 presents this dependency for all the investigated systems. Each value in this figure is obtained by plotting shear stress versus shear rate in the flow curves, displayed as an individual figure for each surfactant to cosurfactant ratio. The flow curves (Figure S3) revealed that the majority of the systems showed a nonlinear relationship between the shear stress (τ) and the shear rate (γ), which is a

DOI: 10.1021/acsomega.8b01272
ACS Omega 2018, 3, 10999−11008

characteristic of a non-Newtonian flux material. Nevertheless, at high shear rates, all the samples exhibit Newtonian behavior; thus, in order to simplify the further discussions, the viscosity at high shear rates was taken into consideration.

Figure 4 presents that in general the viscosity behavior as a function of water volume fraction (W_0) appeared to be similar for all the studied ME systems, except for some slight differences that will be explained here. For glycerol-containing formulations (Figure 4a,b), in the region of a low W_0, addition of water increased the viscosity to up to a maximum. At a low water content, where the water is the dispersed phase, further addition of water resulted in growing of the dispersed droplets and formation of clusters within the oil phase, which are sufficiently close to each other to increase the viscosity.[54,64,65] After the maximum point (W_0 = 30−35%), the ME suffered a structural change to a bicontinuous mixture until reaching a deflection point (W_0 = 40−45%) where O/W MEs were formed. Further dilution (W_0 > 50%) resulted in a slow decrease of viscosity and a constant viscosity value of approximately 3 mPa·s for W_0 > 70%, indicating stable MEs composed of individual spherical oil droplets dispersed in the water phase.[66] The oil to surfactant ratio did not influence the rheological behavior of the ME for Tween 20/glycerol = 1:1. However, at Tween 20/glycerol = 2:1 as shown in Figure 4b, a higher oil to surfactant ratio induced an increase in viscosities of the samples at a lower W_0. The glycerol-free system (Figure 4c) behaved differently at a low W_0, showing almost constant viscosity that could be due to a higher colloidal stability of this system in comparison to the other two, as already observed. Because of that, the deflection point in glycerol-free ME occurred at a much higher W_0. Similar to the other two systems, the oil to surfactant ratio did not influence the rheological behavior of the samples at W_0 > 70%.

In Figure 4c′, the effect of W_0 on the viscosity of the glycerol-free system was studied at a higher temperature (37 °C) to simulate the conditions under which the nanodroplets possibly will be consumed. The behavior at 37 °C showed similar trends as at 25 °C; however, in general, the viscosity was much lower at W_0 < 70%, which is probably due to the increase of oil solubility in water and a further decrease of the interfacial tension in the system, resulting in a drop of the interparticle interactions. At W_0 > 70%, the viscosity turned temperature-independent, as the dilution became the dominating factor. This result suggested that O/W structures are stable at body temperature and may be used as stable vesicles toward the possible delivery points.

Differential scanning calorimetry (DSC) analysis confirmed the structural changes observed by the rheological measurements. In Figure 5, the thermal behavior during cooling of one representative αToc-loaded ME series (ME 121, Table 1) is shown, as a function of W_0. For $W_0 \approx 45$ vol %, the exothermic crystallization peak of the water was not detected upon cooling, meaning that the water was encapsulated strongly by the surfactant/cosurfactant mixture, binding strongly with the hydroxyl groups of glycerol and the ethoxylated groups of Tween 20. This peak was observed for W_0 > 45 vol %, and it shifted from −40 to −14.5 °C as W_0 increased, indicating the structural changes toward the bicontinuous emulsion and the presence of free water molecules with the dilution. For W_0 > 66%, the exothermic crystallization peak approached the one of pure water, indicating that the water in these MEs is the continuous phase, and O/W MEs are formed. The heat of crystallization also increased, indicating the enrichment of the continuous phase with water.

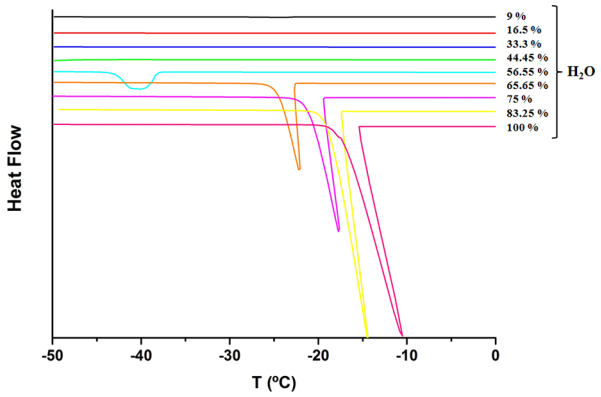

Figure 5. Thermal behavior of all samples of series ME121 with various water contents in αToc-loaded systems.

2.3. Stability of the αToc-Loaded MEs. The stability of two selected αToc-loaded samples, with and without cosurfactant, was assessed by DLS and UV spectroscopy measurements. For most commercial purposes, it is critical that MEs are colloidally stable and the nanodroplets are physically stable all over their shelf-life. To evaluate the capsules' stability, the evolution of the mean particle size over a storage time of 3 months and the corresponding UV spectra of αToc-loaded MEs over 1 month were followed. The average particle size for both cosurfactant-free and cosurfactant-holder systems remained nearly constant during the 3 months of storage period at ambient temperature (Figure S4).

Encapsulated αToc is supposed to be protected against degradation when exposed to ambient conditions. To prove it, UV spectroscopy measurements were performed, as the degradation products absorb at different wavelengths than αToc.[23,46,67] The evolution of the UV spectra for samples 6 and 17 (Table S1) are presented in Figure 6a,b, respectively. The spectra showed the presence of the most important peak characteristics of αToc at 300 nm.[68] The intensity of the peak remained almost constant within the time, and no extra absorption was noticed in the spectra, which confirmed the good chemical stability of the encapsulated αToc.

2.4. Encapsulated αToc Antioxidant Property Assessment. In this study, EPR spectroscopy using a stable nitroxide-free radical ((2,2,6,6-tetramethylpiperidin-1-yl)oxyl) (Tempol) was applied to study the antioxidant properties of the encapsulated αToc. Tempol is characterized by a well-defined EPR spectrum consisting of three peaks (a_N = 16.6 G, g = 2.0078). The antioxidant activity of the corresponding blank ME samples (αToc-free) toward the Tempol stable free radical was first examined and only negligible decreasing of the radical signal was noticed, indicating the absence of any scavenging reaction of IAAc (the oil phase) toward the Tempol radical.

In the presence of encapsulated αToc, the intensity of these peaks in the EPR spectrum of Tempol was decreased because of the scavenging reaction taking place between the stable radical and the antioxidant. In the αToc-loaded MEs, the intensity of the EPR spectra was decreased as the concentration of αToc increases. The corresponding EPR spectra in the absence and presence of different concentrations of αToc are shown in Figure S5. Figure 7 shows the time-dependent Tempol inhibition percentage of the nanodroplets

DOI: 10.1021/acsomega.8b01272
ACS Omega 2018, 3, 10999−11008

Table 1. Composition of αToc-Loaded ME Formulations

	formulation					
phase	ME111 (g)	ME121 (g)	ME110 (g)	ME211 (g)	ME221 (g)	ME210 (g)
oil + αToc	0.3	0.3	0.3	0.6	0.6	0.6
surfactant	1.35	1.8	2.7	1.35	1.8	2.7
cosurfactant	1.35	0.9	0	1.35	0.9	0
water	0.3−0.6−1.5−2.4−3.9−5.7−9.0−15.0					

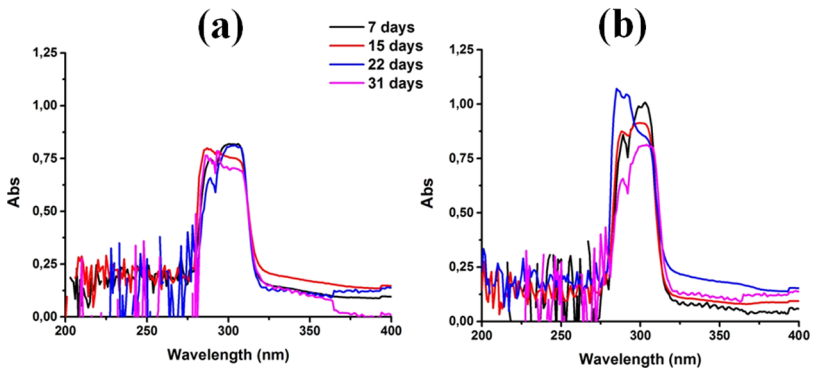

Figure 6. Stability data: evolution of UV spectra during 1 month of cosurfactant containing ME (a) and cosurfactant-free ME (b).

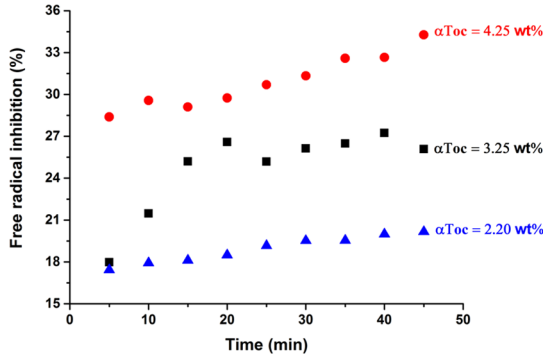

Figure 7. Scavenging effect of encapsulated different concentrations of αToc on Tempol-free radical as a function of incubation time using EPR spectroscopy.

with different concentrations of αToc. As it can be seen in this figure, the amount of loaded αToc significantly influences its inhibition activity. The inhibition did not decrease in time, as it may be expected for not encapsulated αToc; even more, the inhibition rather increased, which may be an indication of a spontaneous slow release of αToc because of changes in the medium during sample preparation.

3. CONCLUSIONS

In this work, an αToc antioxidant compound was encapsulated within nanodroplets created by ME media using completely food-grade components for possible application as additives in food and beverages. Three different oils (lemon oil, IPPM, and IAAc), Tween 20 as the surfactant, and glycerol as the cosurfactant were investigated as the ingredients. A cosurfactant-free system was studied in order to determine the possibility of elimination of this component from the ME formulations.

Among the studied oils in αToc-free MEs, IAAc was selected as the most appropriate one in terms of good compatibility with all the other components. Using the selected IAAc oil, the MEs were loaded with αToc, and the influence of the most important parameters on the formation of MEs was studied (Tween 20 to glycerol ratio; oil to surfactant ratio, and water content). The structural changes in the pseudobinary mixtures were followed by determining the phase behavior in the system, particle size measurements, rheology, and DSC measurements. The concentration ranges of the ME components were determined where preferentially W/O, binary, or O/W MEs were created and also the ranges of the investigated parameters where the desired O/W MEs were formed. The average size of the droplets was in the range of 8.38−19.21 nm. Further studies were carried out on selected colloidally stable O/W αToc-loaded MEs, one of which contained glycerol and the second one glycerol-free, and their stability and radical scavenging activities were determined.

The stability studies performed by following the average droplet size and measuring the UV spectra within the time of storage have shown that the nanodroplets did not significantly change the size and that there was no new absorption peak created in the UV spectra, whereas the characteristic peak of αToc was kept without significant changes, demonstrating chemical and colloidal stability.

Using EPR spectra measurements in the presence of stable Tempol radicals, it was demonstrated that the nanodroplets have radical scavenging activities, which was retained and even increased during the measurement time, which demonstrates the slow releasing of αToc from the nanodroplets.

This work is a proof of concept of the use of MEs to prepare fully food-grade nanodroplets containing bioactive ingredients, without any utilization of high-energy equipment that characterized it by reduced process costs and easier scaling-up. The results from this study might provide an innovative applied technique in the area of pharmaceutical and functional foods.

4. EXPERIMENTAL SECTION

4.1. Materials. αToc (≥96%), lemon oil (California origin), IPM (≥98%), IAAc (≥95%), Tween 20 BioXtra and the free radical Tempol were purchased from Sigma-Aldrich. The vegetable glycerol was purchased from Essential Depot.

DOI: 10.1021/acsomega.8b01272
ACS Omega 2018, 3, 10999−11008

4.2. Selection of Oil. The procedure to select the suitable oil for the developing of ME was based on a pseudoternary phase diagram preparation that revealed the phase behavior of the system. The three different studied food-grade oils were as follows: lemon oil, IPM, or IAAc.

The O/W MEs consisted of water, oil, and surfactant Tween 20 (HLB = 16.7), and glycerol was used as a cosurfactant and it was compared with the cosurfactant-free ME systems with the aim of replacing a certain proportion of the surfactant. The phase behavior of the blank MEs without αToc was determined by pseudoternary phase diagrams. Initially, the mixtures of the oil phase and the surfactant phase (either with or without cosurfactant) of six different fixed weight ratios (3:2, 9:5, 9:4, 1:3, 2:9, and 1:9) were accurately weighed and put into six glass beakers. The different ratios between the surfactant and the cosurfactant were 1:1, 2:1, and 1:0, respectively. The samples in each beaker were mixed homogeneously using a magnetic stirrer for 30 min until oily liquid mixtures were obtained at room temperature. Then, using the water titration method, aliquots of ultrapure water were slowly added drop-by-drop into each oily mixture at room temperature. After addition of each aliquot, mixtures were kept under stirring for a sufficiently long time (from a few hours to 24 h) to attain equilibrium. Phase separations were detected visually by the appearance of cloudiness or sharply defined separated phases. The mixture was determined as stable ME when it had a clear and stable appearance and moreover when it showed a unimodal, average droplet size of <100 nm in DLS measurements. OriginPro 9.0 was used to draw the pseudoternary phase diagram. Obviously, a fixed (weight, volume, or mole) ratio must be chosen for any two of the components and one of the triangle vertices represents 100% of this binary mixture. All the selected MEs were stored at room temperature and the stability of each sample was assessed by inspection in terms of visual clarity and droplet size over time. The oil that produced the largest regions of stable ME in pseudoternary phase diagrams was selected for further investigation for αToc encapsulation.

4.3. Formulation and Preparation of αToc-ME. On the basis of different ratios between the surfactant and the cosurfactant (1:1, 2:1 and 1:0) plus different ratios between the oil phase and the surfactant phase (1:9 and 2:9), six formulations of αToc-ME (Table 1) containing a fixed proportion of αToc dissolved in the oil phase (50 wt %) were prepared. From each formulation, eight duplicates were made and eight different quantities of water as written in Table 1, (last row) were added to them. The obtained 48 mixtures were stirred for 48 h at 25 °C under light shielding. Similar to the previous section, the ME regions were determined by plotting pseudoternary phase diagrams.

4.4. Droplet Size Measurements. Droplet size distributions of MEs were measured using a DLS instrument (Zetasizer Nano S, Malvern Instruments, Malvern, UK). This instrument determines the droplet size from intensity−time fluctuations of a laser beam (633 nm) scattered from a sample at an angle of 173°. The final value of average droplet size (droplet diameter) is a *z*-average of three measurements that were analyzed in 13 runs of 30 s each. To avoid multiple scattering effects, the samples were diluted before the droplet size measurements using ultrapure water. All measurements were conducted at 25 °C after overnight storage of the clear samples.

4.5. Stability Studies. The stability of two selected αToc-loaded samples, both kept under N_2 and light-shielded, was assessed by two techniques. First by DLS, the mean droplet size diameter and PDI of the samples were measured after 1 night of storage and repeated every month for a total period of 3 months. Second, the stability of encapsulated αToc was studied using a UV-2550PC UV spectrophotometer (Shimadzu) by weekly intervals for a month. Therefore, the absorption spectra of the respective ME were measured in the 200−800 nm wavelength range. For both the methods, the samples were prepared by dilution of the MEs in distilled water. Distilled water was used as a reference in the UV spectroscopy analysis.

4.6. EPR Measurements. EPR measurements were performed at constant 25 °C, using a Bruker ELEXSYS 500 spectrometer operating at the X-band. The spectrometer was equipped with a superhigh-Q resonator ER-4123-SHQ and the samples were placed into an EPR flat cell. Typical instrument settings were: center field, 3485 G; scan range, 200 G; gain, 6.3×10^2; time constant, 81.92 ms; modulation amplitude, 0.2 microwave power, 2 mW. The data were collected and processed using the Bruker Xepr suite. The experimental protocol was as follows: in order to standardize the EPR method, samples with three different concentrations of αToc (4.16, 3.33, and 2.17 wt %) were prepared as explained before. Then, the appropriate amount of Tempol was added, to reach the final concentration of 0.1 M. The mixture was stirred and instantly transferred into an EPR flat cell for analysis. The EPR spectra were recorded for 45 min at 25 °C. The inhibition percentage of the corresponding EPR spectrum was obtained from the following equation and plotted as a function of time[49]

$$\text{Inhibition (\%)} = [(A_{\text{Ref}} - A_{\text{sample}})\, A_{\text{Ref}}] \times 100 \quad (1)$$

where A_{Ref} is the integral intensity of the EPR spectrum of the reference sample (Tempol solution with αToc-free ME) and A_{sample} is the integral intensity of the EPR spectrum in the presence of the loaded system.

4.7. Morphological Evaluation. FEI Tecnai G2 20 TWIN TEM was used to study the morphology of αToc-ME. Two selected samples were prepared by placing a drop of diluted ME samples onto a film-coated copper grid; then, they were stained with a drop of 2% aqueous solution of phosphotungstic acid, and finally they were left at room temperature to be dried before testing.

4.8. Viscosity Measurements. The influence of the oil content, the ratio between the surfactant and the cosurfactant, and temperature on the viscosity of αToc-ME was determined using a Physica MCR101 rotational rheometer from Anton Paar GmbH (Graz, Austria), with a concentric cylinder measuring system (10.836 mm diameter cup and 9.998 mm diameter bob). The rheological behavior of each disperse system was examined by plotting the shear stress (σ) versus the shear rate ($\dot{\gamma}$) values. Those systems that showed proportionality in both parameters (r^2 values > 0.99) were considered to be Newtonian fluids and their viscosity (η) was determined from the slope of the aforementioned curve. All other systems were assumed to be non-Newtonian fluids and their viscosity values were obtained by the viscometer at the highest shear rate (1000 S^{-1}). Measurements were obtained at 25 °C and in order to see the effect of temperature on one hand and on the other to simulate the body temperature, one series of MEs has been tested at 37 °C as well. Reproducibility (triplicate) was checked for the samples and no significant differences (±standard deviation) were observed.

DOI: 10.1021/acsomega.8b01272
ACS Omega 2018, 3, 10999−11008

4.9. DSC Measurements. The thermal behavior of the water phase of the MEs was determined using DSC 3+ Mettler Toledo (Greifensee, Switzerland), weighing 4−8 mg of ME samples on a Mettler M3 microbalance, in standard 40 μL aluminum pans, immediately sealed by a press. The samples were cooled in liquid nitrogen from +40 to −50 °C at 10 °C min^{-1}. Each sample remained at this temperature for 2 min and was then heated at a rate of 10 °C min^{-1} to +40 °C. An empty pan was used as a reference.

■ ASSOCIATED CONTENT

Supporting Information

The Supporting Information is available free of charge on the ACS Publications website at DOI: 10.1021/acsomega.8b01272.

Pseudoternary phase behaviors at 25 °C of all the systems investigated in this work: for different oil phases (IPM; lemon oil; IAAc) and different surfactant to cosurfactant ratios (1:1; 2:1; and 1:0); images presenting the visual appearance and the composition of all ME samples loaded with αToc; composition of stable αToc-ME formulations, their droplet size, and PDI; rheological behavior of the cosurfactant-free system; colloidal stability data of the ME with and without the cosurfactant at room temperature over a storage time of 3 months; and EPR spectra in the absence and presence of the cosurfactant at different αToc concentrations (PDF)

■ AUTHOR INFORMATION

Corresponding Author

*E-mail: radmila.tomovska@ehu.es (R.T.).

ORCID

M. Ali Aboudzadeh: 0000-0001-8829-8072

Radmila Tomovska: 0000-0003-1076-7988

Notes

The authors declare no competing financial interest.

■ ACKNOWLEDGMENTS

The Basque Government (GV IT999-16 and Ekartek KK-2017/00015), the Spanish Government (CTQ2016-80886-R), and NATO (SfP project G4255) are gratefully acknowledged for their financial support.

■ REFERENCES

(1) Mcclements, D. J.; Decker, E. A.; Park, Y.; Weiss, J. Structural Design Principles for Delivery of Bioactive Components in Nutraceuticals and Functional Foods. *Crit. Rev. Food Sci. Nutr.* **2009**, *49*, 577−606.

(2) Samaniego-Vaesken, M. d. L.; Alonso-Aperte, E.; Varela-Moreiras, G. Vitamin Food Fortification Today. *Food Nutr. Res.* **2012**, *56*, 5459.

(3) Pathakoti, K.; Manubolu, M.; Hwang, H.-M. Nanostructures: Current Uses and Future Applications in Food Science. *J. Food Drug Anal.* **2017**, *25*, 245−253.

(4) Roohinejad, S.; Oey, I.; Wen, J.; Lee, S. J.; Everett, D. W.; Burritt, D. J. Formulation of Oil-in-Water β-Carotene Microemulsions: Effect of Oil Type and Fatty Acid Chain Length. *Food Chem.* **2015**, *174*, 270−278.

(5) Mayer, S.; Weiss, J.; McClements, D. J. Behavior of Vitamin E Acetate Delivery Systems under Simulated Gastrointestinal Conditions: Lipid Digestion and Bioaccessibility of Low-Energy Nanoemulsions. *J. Colloid Interface Sci.* **2013**, *404*, 215−222.

(6) Walker, R.; Decker, E. A.; McClements, D. J. Development of Food-Grade Nanoemulsions and Emulsions for Delivery of Omega-3 Fatty Acids: Opportunities and Obstacles in the Food Industry. *Food Funct.* **2015**, *6*, 41−54.

(7) Tao, J.; Zhu, Q.; Qin, F.; Wang, M.; Chen, J.; Zheng, Z.-P. Preparation of Steppogenin and Ascorbic Acid, Vitamin E, Butylated Hydroxytoluene Oil-in-Water Microemulsions: Characterization, Stability, and Antibrowning Effects for Fresh Apple Juice. *Food Chem.* **2017**, *224*, 11−18.

(8) Xu, Z.; Jin, J.; Zheng, M.; Zheng, Y.; Xu, X.; Liu, Y.; Wang, X. Co-Surfactant Free Microemulsions: Preparation, Characterization and Stability Evaluation for Food Application. *Food Chem.* **2016**, *204*, 194−200.

(9) He, J.; Zhu, Q.; Dong, X.; Pan, H.; Chen, J.; Zheng, Z.-P. Oxyresveratrol and Ascorbic Acid O/W Microemulsion: Preparation, Characterization, Anti-Isomerization and Potential Application as Antibrowning Agent on Fresh-Cut Lotus Root Slices. *Food Chem.* **2017**, *214*, 269−276.

(10) Shah, A. V.; Desai, H. H.; Thool, P.; Dalrymple, D.; Serajuddin, A. T. M. Development of Self-Microemulsifying Drug Delivery System for Oral Delivery of Poorly Water-Soluble Nutraceuticals. *Drug Dev. Ind. Pharm.* **2017**, *44*, 895−901.

(11) Yaghmur, A.; de Campo, L.; Aserin, A.; Garti, N.; Glatter, O. Structural Characterization of Five-Component Food Grade Oil-in-Water Nonionic Microemulsions. *Phys. Chem. Chem. Phys.* **2004**, *6*, 1524−1533.

(12) McClements, D. J. Nanoemulsions versus Microemulsions: Terminology, Differences, and Similarities. *Soft Matter* **2012**, *8*, 1719−1729.

(13) Singh, H. Review Article Nanotechnology Applications in Functional Foods; Opportunities and Challenges. *Prev. Nutr. Food Sci.* **2016**, *21*, 1−8.

(14) Komaiko, J. S.; Mcclements, D. J. Formation of Food-Grade Nanoemulsions Using Low-Energy Preparation Methods: A Review of Available Methods. *Compr. Rev. Food Sci. Food Saf.* **2016**, *15*, 331−352.

(15) Herrera, E.; Barbas, C. Vitamin E: Action, Metabolism and Perspectives. *J. Physiol. Biochem.* **2001**, *57*, 43−56.

(16) Brigelius-Flohé, R.; Traber, M. G. Vitamin E: Function and Metabolism. *Fed. Am. Soc. Exp. Biol. J.* **1999**, *13*, 1145−1155.

(17) Galli, F.; Azzi, A.; Birringer, M.; Cook-Mills, J. M.; Eggersdorfer, M.; Frank, J.; Cruciani, G.; Lorkowski, S.; Özer, N. K. Vitamin E: Emerging Aspects and New Directions. *Free Radical Biol. Med.* **2017**, *102*, 16−36.

(18) Traber, M. G.; Atkinson, J. Vitamin E, Antioxidant and Nothing More. *Free Radical Biol. Med.* **2007**, *43*, 4−15.

(19) Sen, C. K.; Khanna, S.; Roy, S. Tocotrienols: Vitamin E Beyond Tocopherols. *Life Sci.* **2006**, *78*, 2088−2098.

(20) Raederstorff, D.; Wyss, A.; Calder, P. C.; Weber, P.; Eggersdorfer, M. Vitamin E Function and Requirements in Relation to PUFA. *Br. J. Nutr.* **2015**, *114*, 1113−1122.

(21) Wang, X.; Quinn, P. J. Vitamin E and Its Functions in Membranes. *Prog. Lipid Res.* **1999**, *38*, 309−336.

(22) Young, I. S.; Woodside, J. V. Antioxidants in Health and Disease. *J. Clin. Pathol.* **2001**, *54*, 176−186.

(23) Nhan, P. P.; Hoa, N. K. Effect of Light and Storage Time on Vitamin E in Pharmaceutical Products. *Br. J. Pharmacol. Toxicol.* **2013**, *4*, 176−180.

(24) Trebst, A.; Depka, B.; Holländer-Czytko, H. A Specific Role for Tocopherol and of Chemical Singlet Oxygen Quenchers in the Maintenance of Photosystem II Structure and Function in Chlamydomonas Reinhardtii. *FEBS Lett.* **2002**, *516*, 156−160.

(25) Khayata, N.; Abdelwahed, W.; Chehna, M. F.; Charcosset, C.; Fessi, H. Preparation of Vitamin E Loaded Nanocapsules by the Nanoprecipitation Method: From Laboratory Scale to Large Scale Using a Membrane Contactor. *Int. J. Pharm.* **2012**, *423*, 419−427.

(26) Verleyen, T.; Verhe, R.; Huyghebaert, A.; Dewettinck, K.; De Greyt, W. Identification of ??-Tocopherol Oxidation Products in

DOI: 10.1021/acsomega.8b01272
ACS Omega 2018, 3, 10999−11008

Triolein at Elevated Temperatures. *J. Agric. Food Chem.* **2001**, *49*, 1508−1511.
(27) Sabliov, C. M.; Fronczek, C.; Astete, C. E.; Khachaturyan, M.; Khachatryan, L.; Leonardi, C. Effects of Temperature and UV Light on Degradation of α-Tocopherol in Free and Dissolved Form. *J. Am. Oil Chem. Soc.* **2009**, *86*, 895−902.
(28) Laouini, A.; Fessi, H.; Charcosset, C. Membrane Emulsification: A Promising Alternative for Vitamin E Encapsulation within Nano-Emulsion. *J. Membr. Sci.* **2012**, *423*−*424*, 85−96.
(29) Saberi, A. H.; Fang, Y.; McClements, D. J. Fabrication of Vitamin E-Enriched Nanoemulsions: Factors Affecting Particle Size Using Spontaneous Emulsification. *J. Colloid Interface Sci.* **2013**, *391*, 95−102.
(30) Shukat, R.; Relkin, P. Lipid Nanoparticles as Vitamin Matrix Carriers in Liquid Food Systems: On the Role of High-Pressure Homogenisation, Droplet Size and Adsorbed Materials. *Colloids Surf., B* **2011**, *86*, 119−124.
(31) Sharif, H. R.; Goff, H. D.; Majeed, H.; Liu, F.; Nsor-Atindana, J.; Haider, J.; Liang, R.; Zhong, F. Physicochemical Stability of β-Carotene and α-Tocopherol Enriched Nanoemulsions: Influence of Carrier Oil, Emulsifier and Antioxidant. *Colloids Surf., A* **2017**, *529*, 550−559.
(32) Diane, J. M. M.; Burgess, J. Vitamin E Nanoemulsions Characterization and Analysis. *Int. J. Pharm.* **2014**, *465*, 455−463.
(33) Suntres, Z. E. Liposomal Antioxidants for Protection against Oxidant-Induced Damage. *J. Toxicol.* **2011**, *2011*, 1−16.
(34) Laouini, A.; Charcosset, C.; Fessi, H.; Holdich, R. G. G.; Vladisavljević, G. T. Preparation of Liposomes: A Novel Application of Microengineered Membranes - Investigation of the Process Parameters and Application to the Encapsulation of Vitamin E. *RSC Adv.* **2013**, *3*, 4985−4994.
(35) Byun, Y.; Hwang, J. B.; Bang, S. H.; Darby, D.; Cooksey, K.; Dawson, P. L.; Park, H. J.; Whiteside, S. Formulation and Characterization of α-Tocopherol Loaded Poly E{open}-Caprolactone (PCL) Nanoparticles. *LWT–Food Sci. Technol.* **2011**, *44*, 24−28.
(36) Chen, C.-C.; Wagner, G. Vitamin E Nanoparticles For Beverage Applications. *Chem. Eng. Res. Des.* **2004**, *82*, 1432.
(37) Reboul, E.; Richelle, M.; Perrot, E.; Desmoulins-Malezet, C.; Pirisi, V.; Borel, P. Bioaccessibility of Carotenoids and Vitamin E from Their Main Dietary Sources. *J. Agric. Food Chem.* **2006**, *54*, 8749−8755.
(38) Feng, J.-L.; Wang, Z.-W.; Zhang, J.; Wang, Z.-N.; Liu, F. Study on Food-Grade Vitamin E Microemulsions Based on Nonionic Emulsifiers. *Colloids Surf., A* **2009**, *339*, 1−6.
(39) He, C.-X.; He, Z.-G.; Gao, J.-Q. Microemulsions as Drug Delivery Systems to Improve the Solubility and the Bioavailability of Poorly Water-Soluble Drugs. *Expert Opin. Drug Delivery* **2010**, *7*, 445−460.
(40) Tirumalasetty, P. P.; Eley, J. G. Permeability Enhancing Effects of the Alkylglycoside, Octylglucoside, on Insulin Permeation across Epithelial Membrane in Vitro. *J. Pharm. Pharm. Sci.* **2006**, *9*, 32−39.
(41) Lin, C.-C.; Lin, H.-Y.; Chi, M.-H.; Shen, C.-M.; Chen, H.-W.; Yang, W.-J.; Lee, M.-H. Preparation of Curcumin Microemulsions with Food-Grade Soybean Oil/lecithin and Their Cytotoxicity on the HepG2 Cell Line. *Food Chem.* **2014**, *154*, 282−290.
(42) Gupta, S. Biocompatible Microemulsion Systems for Drug Encapsulation and Delivery. *Curr. Sci.* **2011**, *101*, 174−188.
(43) Malik, M. A.; Wani, M. Y.; Hashim, M. A. Microemulsion Method: A Novel Route to Synthesize Organic and Inorganic Nanomaterials. *Arabian J. Chem.* **2012**, *5*, 397−417.
(44) Ziani, K.; Fang, Y.; McClements, D. J. Encapsulation of Functional Lipophilic Components in Surfactant-Based Colloidal Delivery Systems: Vitamin E, Vitamin D, and Lemon Oil. *Food Chem.* **2012**, *134*, 1106−1112.
(45) Matsuoka, J.; Kusano, T.; Kasama, Y.; Tominaga, E.; Kobayashi, J.; Fujii, W.; Iwase, H.; Shibayama, M.; Nanbu, H. Structure of the Microemulsion of Polyglycerol Polyricinoleate Encapsulating Vitamin E. *J. Oleo Sci.* **2017**, *66*, 1285−1291.
(46) Chiu, Y. C.; Yang, W. L. Preparation of Vitamin E Microemulsion Possessing High Resistance to Oxidation in Air. *Colloids Surf.* **1992**, *63*, 311−322.
(47) Cieśla, J.; Koczańska, M.; Narkiewicz-Michałek, J.; Szymula, M.; Bieganowski, A. Effect of α-Tocopherol on the Properties of Microemulsions Stabilized by the Ionic Surfactants. *J. Mol. Liq.* **2017**, *236*, 117−123.
(48) Tzika, E. D.; Papadimitriou, V.; Sotiroudis, T. G.; Xenakis, A. Antioxidant Properties of Fruits and Vegetables Shots and Juices: An Electron Paramagnetic Resonance Study. *Food Biophys* **2008**, *3*, 48−53.
(49) Papadimitriou, V.; Sotiroudis, T. G.; Xenakis, A.; Sofikiti, N.; Stavyiannoudaki, V.; Chaniotakis, N. A. Oxidative Stability and Radical Scavenging Activity of Extra Virgin Olive Oils: An Electron Paramagnetic Resonance Spectroscopy Study. *Anal. Chim. Acta* **2006**, *573*−*574*, 453−458.
(50) Chaari, M.; Theochari, I.; Papadimitriou, V.; Xenakis, A.; Ammar, E. Encapsulation of Carotenoids Extracted from Halophilic Archaea in Oil-in-Water (O/W) Micro- and Nano-Emulsions. *Colloids Surf., B* **2018**, *161*, 219−227.
(51) Henry, J. V. L.; Fryer, P. J.; Frith, W. J.; Norton, I. T. Emulsification Mechanism and Storage Instabilities of Hydrocarbon-in-Water Sub-Micron Emulsions Stabilised with Tweens (20 and 80), Brij 96v and Sucrose Monoesters. *J. Colloid Interface Sci.* **2009**, *338*, 201−206.
(52) Kaur, G.; Mehta, S. K. Developments of Polysorbate (Tween) Based Microemulsions: Preclinical Drug Delivery, Toxicity and Antimicrobial Applications. *Int. J. Pharm.* **2017**, *529*, 134−160.
(53) Paul, B. K.; Moulik, S. P. Uses and Applications of Microemulsions. *Curr. Sci.* **2001**, *80*, 990−1001.
(54) Garti, N.; Yaghmur, A.; Leser, M. E.; Clement, V.; Watzke, H. J. Improved Oil Solubilization in Oil/water Food Grade Microemulsions in the Presence of Polyols and Ethanol. *J. Agric. Food Chem.* **2001**, *49*, 2552−2562.
(55) Moreno, M. A.; Ballesteros, M. P.; Frutos, P. Lecithin-Based Oil-in-Water Microemulsions for Parenteral Use: Pseudoternary Phase Diagrams, Characterization and Toxicity Studies. *J. Pharm. Sci.* **2003**, *92*, 1428−1437.
(56) Chen, B.; Hou, M.; Zhang, B.; Liu, T.; Guo, Y.; Dang, L.; Wang, Z. Enhancement of the Solubility and Antioxidant Capacity of α-Linolenic Acid Using an Oil in Water Microemulsion. *Food Funct.* **2017**, *8*, 2792−2802.
(57) Genot, C.; Berton, C.; Ropers, M.-H. The Role of the Interfacial Layer and Emulsifying Proteins in the Oxidation in Oil-in-Water Emulsions. In *Lipid Oxidation, Challenges in Food Systems*; Logan, A., Nienaber, U., Pan, X., Eds.; Elsevier Inc., 2013; Chapter 5, pp 177−210.
(58) Warisnoicharoen, W.; Lansley, A. B.; Lawrence, M. J. Nonionic Oil-in-Water Microemulsions: The Effect of Oil Type on Phase Behaviour. *Int. J. Pharm.* **2000**, *198*, 7−27.
(59) Magdassi, S.; Frank, S. G. Formation of Oil in Glycerol/Water Emulsions: Effect of Surfactant Ethylene Oxide Content. *J. Dispersion Sci. Technol.* **1990**, *11*, 519−528.
(60) You, X.; Xing, Q.; Tuo, J.; Song, W.; Zeng, Y.; Hu, H. Optimizing Surfactant Content to Improve Oral Bioavailability of Ibuprofen in Microemulsions: Just Enough or More than Enough? *Int. J. Pharm.* **2014**, *471*, 276−284.
(61) Yu, A.; Wang, H.; Wang, J.; Cao, F.; Gao, Y.; Cui, J.; Zhai, G. Formulation Optimization and Bioavailability After Oral and Nasal Administration in Rabbits of Puerarin-Loaded Microemulsion. *J. Pharm. Sci.* **2011**, *100*, 933−941.
(62) Moulik, S. P.; Paul, B. K. Structure, Dynamics and Transport Properties of Microemulsions. *Adv. Colloid Interface Sci.* **1998**, *78*, 99−195.
(63) Formariz, T. P.; Sarmento, V. H. V.; Silva-Junior, A. A.; Scarpa, M. V.; Santilli, C. V.; Oliveira, A. G. Doxorubicin Biocompatible O/W Microemulsion Stabilized by Mixed Surfactant Containing Soya Phosphatidylcholine. *Colloids Surf., B* **2006**, *51*, 54−61.

DOI: 10.1021/acsomega.8b01272
ACS Omega 2018, 3, 10999−11008

(64) Saidi, Z.; Mathew, C.; Peyrelasse, J.; Boned, C. Percolation and Critical Exponents for the Viscosity of Microemulsions. *Phys. Rev. A: At., Mol., Opt. Phys.* **1990**, *42*, 872−876.
(65) Yaghmur, A.; Aserin, A.; Antalek, B.; Garti, N. Microstructure Considerations of New Five-Component Winsor IV Food-Grade Microemulsions Studied by Pulsed Gradient Spin-Echo NMR, Conductivity, and Viscosity. *Langmuir* **2003**, *19*, 1063−1068.
(66) Djordjevic, L.; Primorac, M.; Stupar, M.; Krajisnik, D. Characterization of Caprylocaproyl Macrogolglycerides Based Microemulsion Drug Delivery Vehicles for an Amphiphilic Drug. *Int. J. Pharm.* **2004**, *271*, 11−19.
(67) Carlotti, M. E.; Rossatto, V.; Gallarate, M. Vitamin A and Vitamin A Palmitate Stability over Time and under UVA and UVB Radiation. *Int. J. Pharm.* **2002**, *240*, 85−94.
(68) Tiburcio-Moreno, J. A.; Marcelín-Jiménez, G.; Leanos-Castaneda, O. L.; Yanez-Limon, J. M.; Alvarado-Gil, J. J. Study of the Photodegradation Process of Vitamin E Acetate by Optical Absorption, Fluorescence, and Thermal Lens Spectroscopy. *Int. J. Thermophys.* **2012**, *33*, 2062−2068.

DOI: 10.1021/acsomega.8b01272
ACS Omega 2018, 3, 10999−11008